

## Electronic Supplementary Information

### Superhydrophobic Coating Fabrication

One part of the bottom coat was diluted in two volume parts acetone and one volume part xylenes. A glass microscope slide surface was fully wetted with 2 mL of the bottom coat mixture. Parameters used for spin coating are provided in Table S1. The final coating was allowed to dry for 1 h at room temperature. To apply a layer of top-coat, one part of UED-top-coat was diluted in two parts of acetone. 2 mL of the mixture was used to fully wet a microscope slide previously coated with bottom coat and the same spinning program was performed. The coating was allowed to dry for 1 h before the chip was used or more layers of top-coat were applied.

**Tab. S1** Spin coating parameters used to apply the UED<sup>®</sup> base and top coat.

Step	Speed / rpm	Accel. / rpm/s	t/s
1	200	5	15
2	0	1200	2
3	200	5	15
4	0	1200	2
5	700	1200	2
Total			36

### SH Surface Fabrication and Characterization

For optimization of the coating procedure different numbers of top coat were applied on one layer of UED<sup>®</sup> base coat. The resulting water-contact-angles (WCA) and coating thicknesses was measured (Fig.S1).

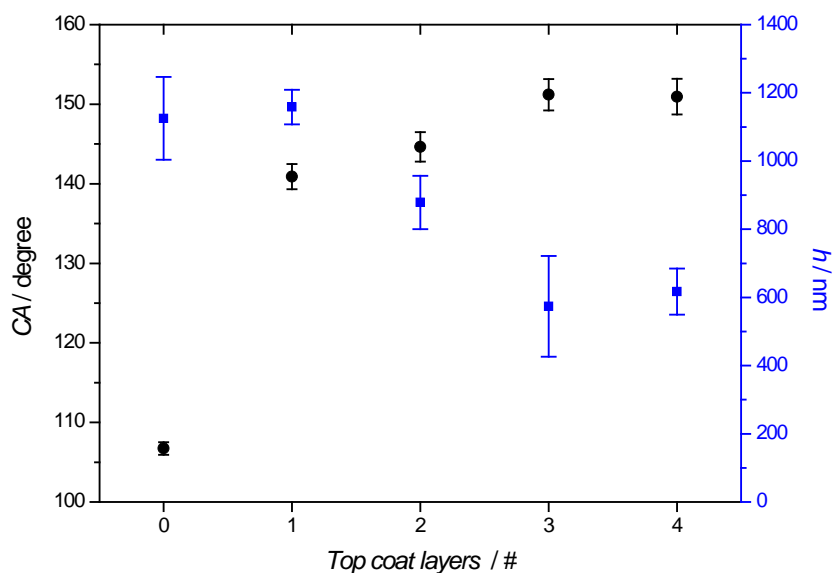


**Fig. S1** WCAs (black circles) and coating thicknesses (blue squares) obtained for spin coated UED<sup>®</sup> slides for different numbers of top-coat layers. On all slides, a layer of base-coat was applied first. The contact angle and thickness at 0 top coat layers represents the CA for the base-coat.

The WCA increases with the number of applied top coat layers until it reaches  $151.2 \pm 2.2^\circ$  for three layers and does not change with application of a fourth layer. Therefore, all superhydrophobic substrates were fabricated by applying three top coat layers.

Interestingly, the overall coating thickness decreases with the number of applied top coat layers. The transparent base coat itself has the highest thickness of  $1125 \pm 122$  nm. Application of four top-coat layers decreases the overall thickness down to  $617 \pm 68$  nm. Application of a fourth top-coat layer does not change the overall thickness compared to three top-coat layers. Such behaviour can be explained with the help of SEM and optical profilometry images (Fig. S2).

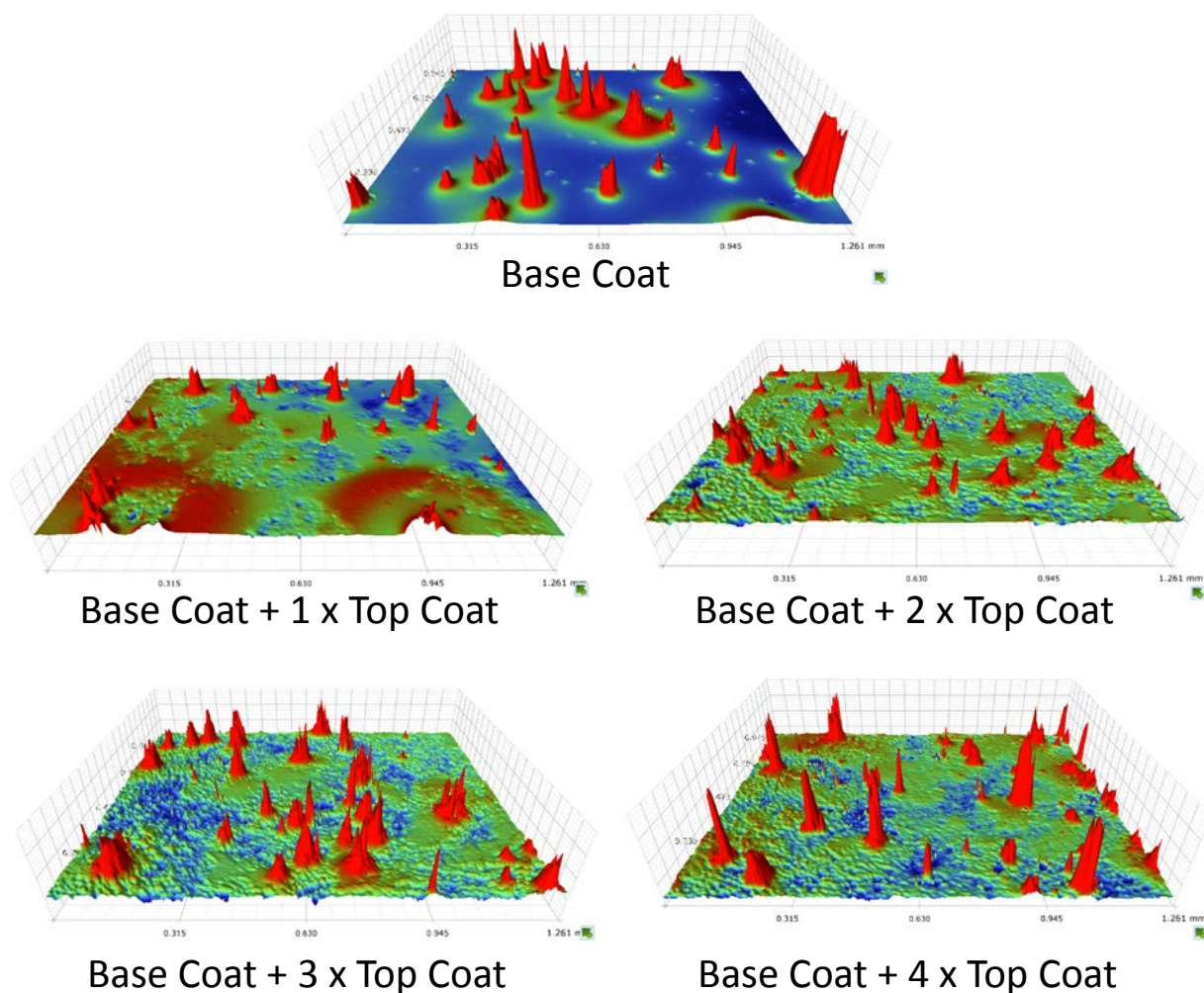


**Fig. S2** Optical surface profilometer images of UED<sup>®</sup> coated slides. The measured area is 1.261mm x 1.261mm. All profiles are taken at the same scale. The tip of red peaks is approximately 20  $\mu$ m.

Optical profilometer images of the base coat show features that are up to 100 $\mu$ m wide (red spikes) on an otherwise smooth surface (blue). Application of the top coat increases the surface roughness by agglomerates that cover the initially smooth surface (blue and green). With increasing number of applied top coats, the initially smooth areas of the base coat become smaller and disappear after application of

three top coats. Profilometer images do not show a change in roughness and topology when more than three top coats are applied. This increase in roughness favours a Cassie/Baxter state and results in higher WCAs.

An overall decrease of the thickness compared to the thickness of the pure base-coat at the beginning means that less base-coat is present when top-coat is applied. This can be explained by the spin coat procedure. For every applied layer of top-coat acetone as a component of the top coat is also applied onto the surface. The base-coat is soluble in acetone. As a result, spinning removes a portion of the base-coat as it flows from the centre to the perimeter of the substrate. At the same time, the increase in roughness is an indication for more top-coat material deposited onto the surface. The surface profile of three top-coat layers placed on a base-coat shows no smooth (blue) areas anymore, what indicates that the surface is fully covered with top-coat. When a fourth layer of top-coat is applied the acetone does not likely contact the base-coat anymore. Therefore, no base-coat is removed, and the thickness stays consistent.

### Air Plasma Treatment for Simultaneous Surface Energy Trap Fabrication

Hydrophilic areas on a superhydrophobic surface of UED<sup>®</sup> can be generated by exposing selected areas to air plasma. This introduces hydroxyl-groups which decrease the WCA of the surface and leads to SETs. A 3D printed mask and mask holder are used to ensure tight contact between the mask and the SH surface (Fig. S3).

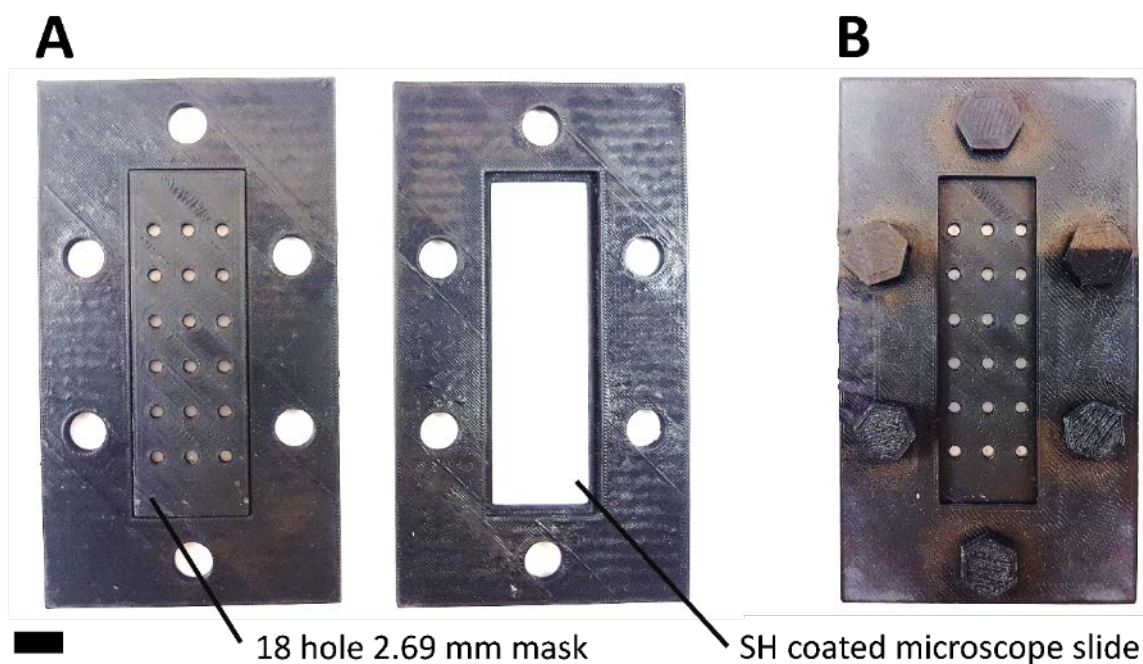


**Fig. S3** 3D printed screw retained frame for alignment of the mask with the substrate. A) disassembled and B) assembled. The scale bar is 10 mm.

## Transparency of SH coatings

The transmittance of UED<sup>®</sup> coated glass slides was investigated with a benchtop UV/VIS spectrometer. The glass slide has in the range of 350-800 nm a transmittance of 90% that drops to 0% for lower wavelengths. Similarly, the transmittance of UED<sup>®</sup> coated slides drops to 0% for low wavelengths and shows an increasing transmittance for higher wavelengths. In the VIS/NIR range (400-800 nm) the average transmittance of 77 % based on five different measurements on one slide with an RSD of 2.2 %.

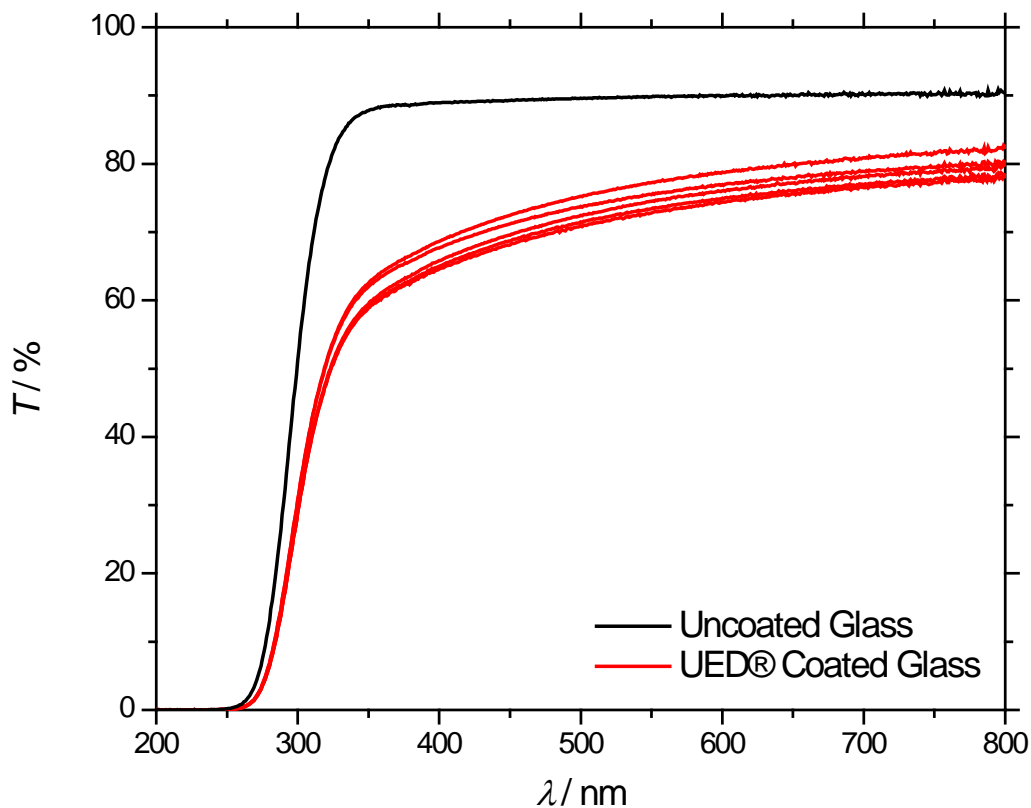


**Fig. S4** Optical Transmittance of an uncoated glass microscope slide that was used as substrate and the transmittance of a glass slide coated with one bottom layer and three top layers of UED<sup>®</sup>. The transmittance for UED<sup>®</sup> coated slides was measured on 5 different spots and have an RSD of 2.2 % in the range between 420-580 nm.

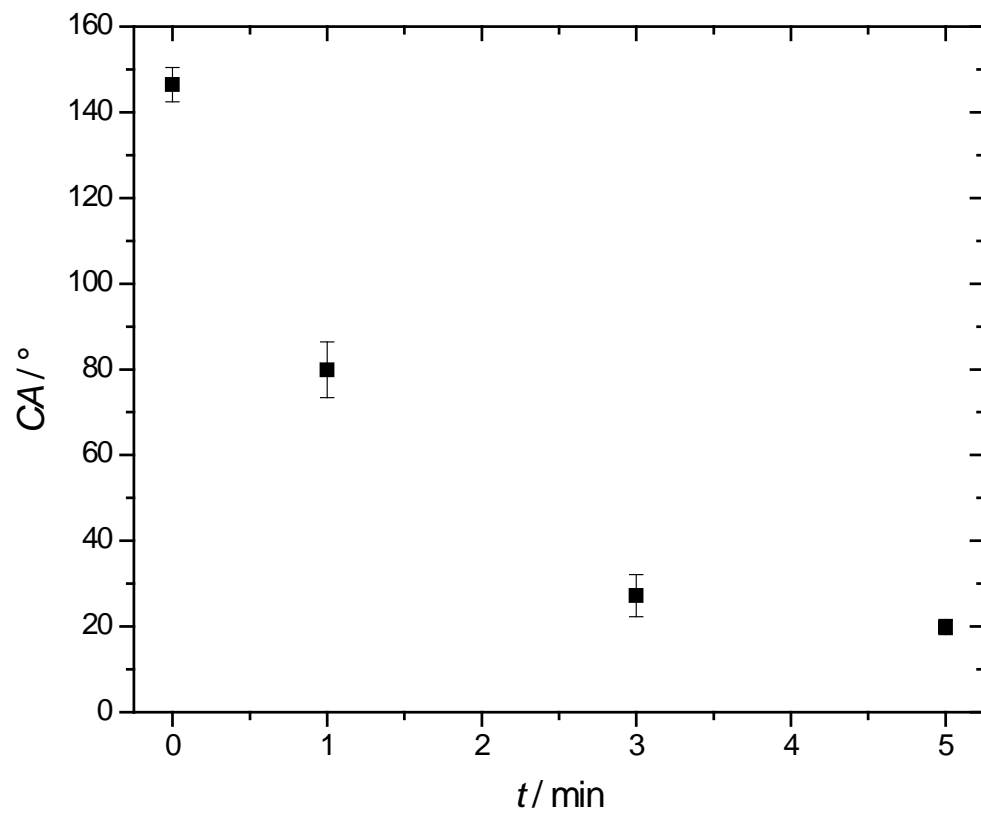


**Fig. S5** Dependence of UED® water contact angle from the plasma treatment time.

### Laser Micromachining for Sequential Surface Energy Trap Fabrication

Laser micromachined SETs were fabricated by ablating a circle of the superhydrophobic coating. Bachus *et al.*<sup>1</sup> have shown that hydrophilicity is not just present at the spots that were hit by the laser, but also in the region around which is called the mill broadening zone.

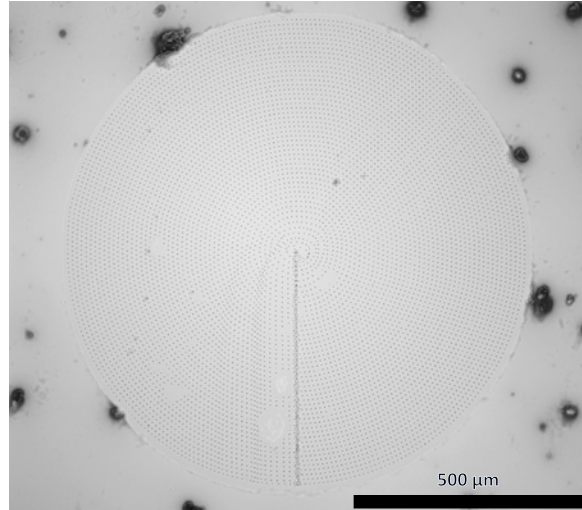


**Fig. S6** Laser micromachined SET with a diameter of 1mm. The dark spots show where the laser ablated parts of the superhydrophobic coating to generate hydrophilicity. The mill broadening is visible and about 25μm wide.

### 3D-Printed Memory Foam Lifting Device

To ensure reproducible lifting speeds of the top SET a 3D-printed slide lifting device based on memory foam was designed. The bottom slide is placed inside the device and the top slide sits on a frame which is placed on two pieces of memory foam.

This allows one to push the top SH-chip downwards against the memory foam until it is in contact with the top phase of the droplet. A spacer ensures that droplets are not excessively squished. Releasing the top chip causes the memory foam to uniformly expand. The lifting speed (5mm/s) is controlled by the memory foams expansion time and independent of the user.

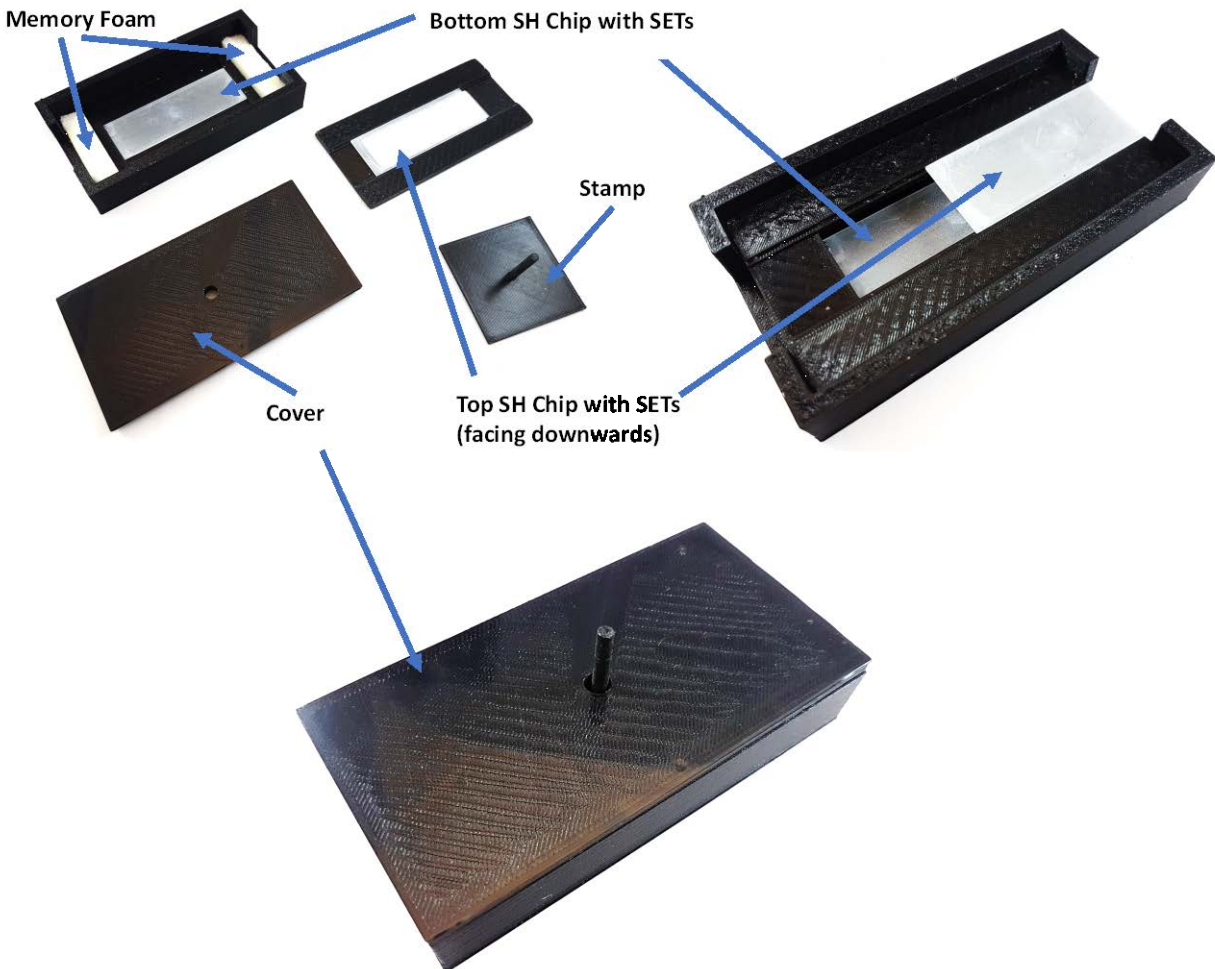


**Fig. S7** 3D-printed memory foam lifting device to ensure consistent lifting speed of the top slide.



## Phase separation time

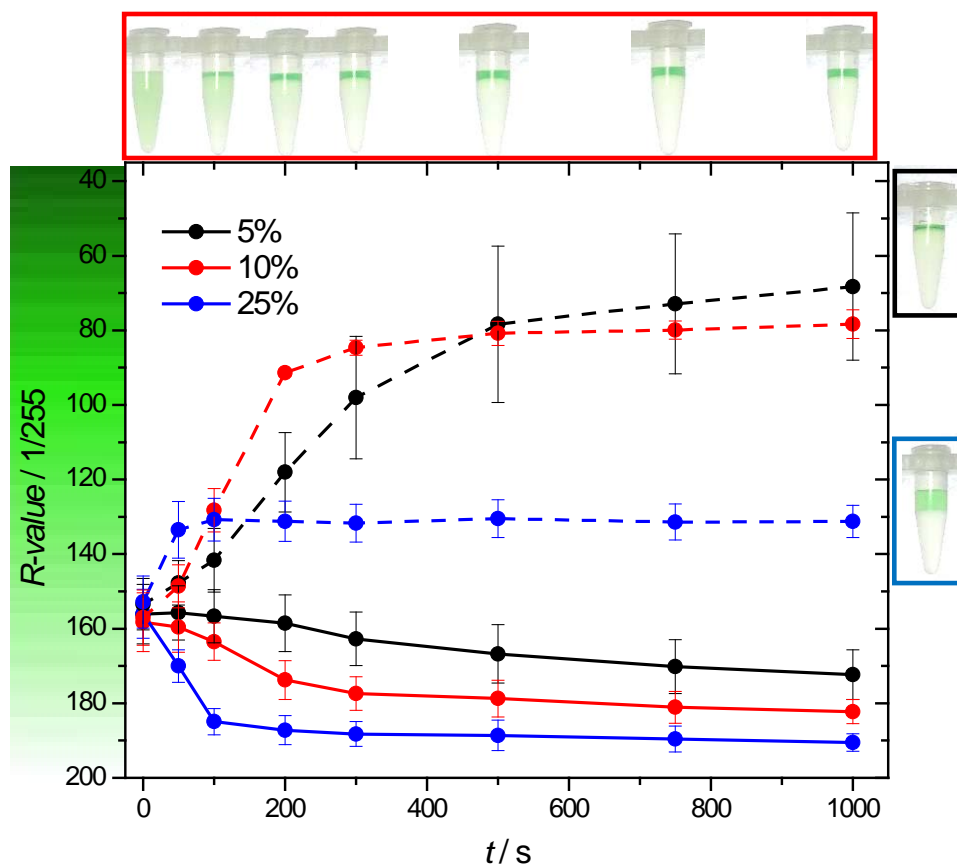


**Fig. S8** Phase separation times of an ATPS in a vial with a total volume of 1.5 mL. ATPS with three different PEG volume fractions (5%, 10% and 25%) were investigated. A lower R-value corresponds to a darker hue of green while a higher R-value corresponds to a lighter green. The dashed lines correspond to the R-values of the upper PEG phase and the solid lines to the R-values to the lower  $\text{Na}_2\text{SO}_4$  phase.



## Smartphone based VIS Spectrometer

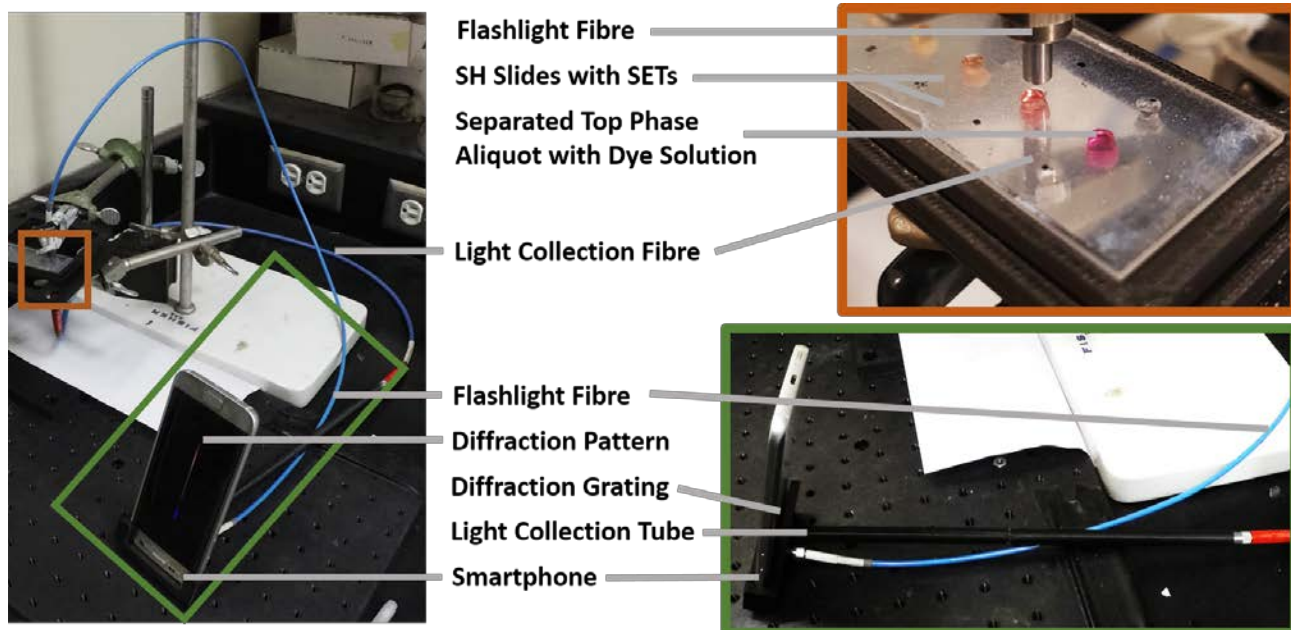


**Fig. S9** The picture on the left shows the full setup of the portable VIS spectrometer. A closeup of the smartphone holder with the smartphone, diffraction grating, light collection tube and connection for the flashlight fibre is shown at the bottom right. The flashlight fibre leads the light to a separated aliquot of the top phase that is dyed and placed between two SETs (top right). A light collection fibre is placed underneath the sample and leads the emitted light to the light collection tube of the smartphone holder.

Two optical bandpass filters (ET470/40, Nikon and ET620/60, Nikon) were used for calibration. By determining the edges of the transmitted wavelength each bandpass filter provided two calibration points that were used in Figure S10.

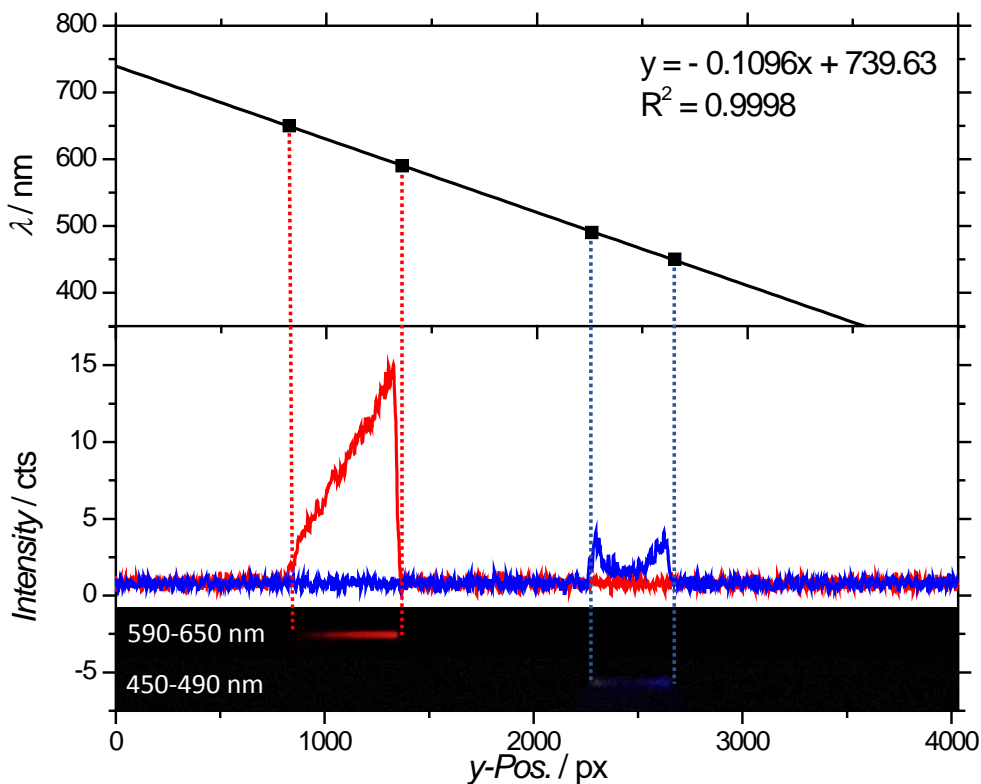


**Fig. S10** Two optical bandpass filters were used to calibrate the pixel position along the diffraction pattern to the according wavelength. A bandpass filter was placed in the spectrometer and illuminated using the flashlight. The range of the bandpass filter is known and can be correlated to the positions were measured intensity drops. Two different bandpass filters allowed us to determine four calibration points.

Each spectrum shows the characteristic emission of a phosphor-converted white LED that was used as illumination source. The emission spectra of such LEDs have a peak around 450 nm from the InGaN/GaN-LED and a broad peak in the range between 500 and 650 nm caused by Stokes shifted light from phosphor. The LED's low emission intensity around 470 nm does not allow absorption measurements in that range. However, in this application that region does not fall in a region of interest.

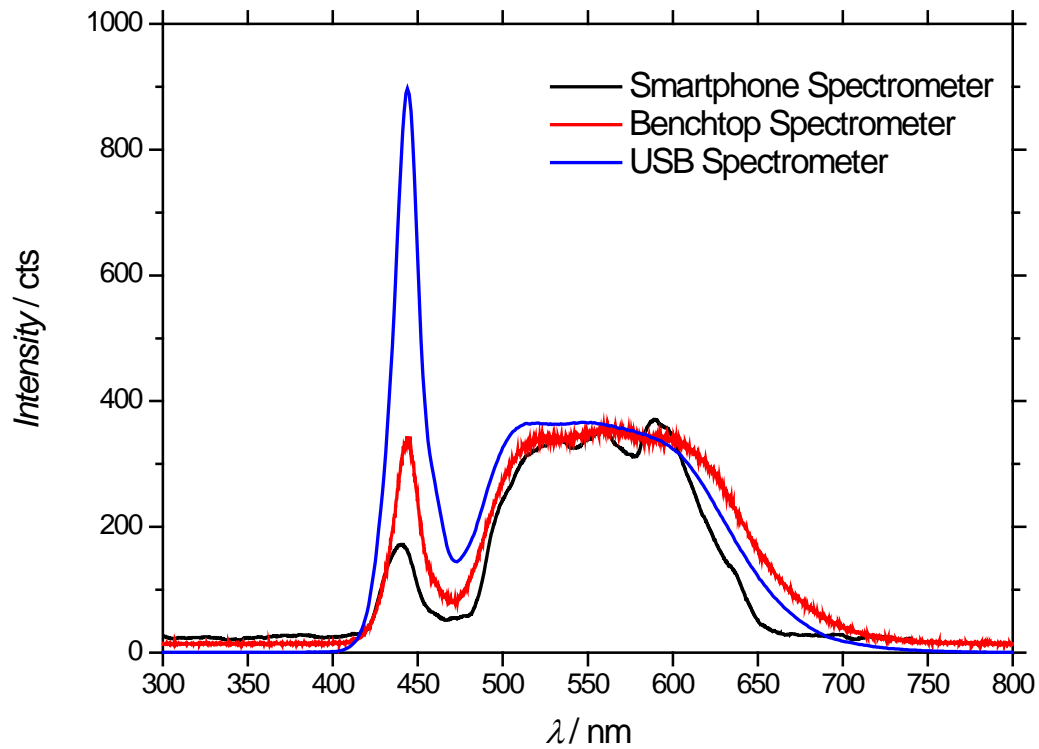


**Fig. S11** The developed smartphone-based spectrometer was compared to a benchtop spectrometer and a portable USB spectrometer. With each spectra of the used flashlight were taken with each spectrometer. All spectrometers can record the characteristic emission spectrum of a phosphor-converted white LED that shows a peak of the GaN or InGaN LED around 440 nm. Additionally, the part the LEDs emitted light is stoke shifted by added phosphor and causes a broad peak in the range between 500 -700 nm.

### Calibration Curve Concentration Series

To show that an interference free determination of cadmium is possible and that normalization of obtained spectra by using the ratio of two wavelengths (445/535 nm) eliminates the impact of varying illumination intensities a calibration curve was measured based on 5 different cadmium concentration series. The concentration series differ in the metals the sample contain (just Cd<sup>2+</sup> or Mn<sup>2+</sup>, Ni<sup>2+</sup>, Cu<sup>2+</sup>, Pb<sup>2+</sup>, Fe<sup>3+</sup>, Cd<sup>2+</sup>), the exposure time images were taken and if a closed (two slide) setup with well-defined light path length or an open (one slide) setup was used.

**Table S2** Five different extraction series were used to obtain a calibration curve. The column Metal Ions shows if just cadmium (Cd) or a mix of metals (Mix) was in the sample, the column exposure time lists the used exposure time of the smartphone camera in manual mode and Setup shows whether a closed setup with two slides or an open setup with just one slide was used.

No	Metal Ions	Exposure Time / s	Setup
1	Cd	1/350	Open
2	Cd	1/250	Closed
3	Mix	1/250	Open
4	Mix	1/180	Closed
5	Mix	1/180	Open

### References

- 1 K. J. Bachus, L. Mats, H. W. Choi, G. T. T. Gibson and R. D. Oleschuk, *ACS Appl. Mater. Interfaces*, 2017, **9**, 7629–7636.